Dynamics of the Structure of the Atmosphere Over Mountainous Terrain From 4-70 KM as Inferred From High-Altitude Chaff, Ozone Sensors and Supper-Pressure Balloons

By
James E. Lovill

Department of Atmospheric Science
Colorado State University
Fort Collins, Colorado

Colorado State University

Department of Atmospheric Science

DYNAMICS OF THE STRUCTURE OF THE ATMOSPHERE OVER MOUNTAINOUS TERRAIN FROM 4-70 KM AS INFERRED FROM HIGH-ALTITUDE CHAFF, OZONE SENSORS AND SUPER-PRESSURE BALLOONS

by

James E. Lovill

Atmospheric Science Paper No. 160

Department of Atmospheric Science
Colorado State University
Fort Collins, Colorado

January 1970

ABSTRACT

A project was conducted during September 1969 to determine the structure of the atmosphere over the Colorado Rocky Mountains from 4-70 km. Chaff was ejected from gun projectiles at 60-70 km altitude. Superpressure balloons were flown in the mid- and upper-troposphere. Ozone sensors were flown to heights of 37 km.

Wave motion appears to be evident in the mesospheric chaff data. A spectral analysis is performed on the components of motion of the chaff to determine primary modes. A velocity of 53 m s^{-1} and vertical shear of 35 m s^{-1} km^{-1} were recorded in the mid-mesosphere. There is a slight suggestion that the autumn high-altitude wind reversal might have occurred in thin layers, since thin layers of easterlies embedded in a basic westerly flow were seen the last of September. Wave motion is also evident in the superpressure balloon data. Four ozonesondes were released at three-hour intervals. During that twelve-hour period, the ozonesonde data indicated that strong gravity waves were present and that they were nearly stationary. A maximum of ozone at 6 km was seen during the quasi-stationary gravity wave episode. The maximum corresponded to 1) a low-level velocity maximum of 26 m s^{-1}, 2) a region of vertical convergence, and 3) a temperature inversion. Continuous surface ozone data were obtained at the mountain ozonesonde release site. Maximum ozone concentrations were found in the early morning hours and minimum concentrations in the early afternoon. The possible processes that produce this fluctuation are discussed.

TABLE OF CONTENTS

Table of Contents Continued

LIST OF FIGURES AND TABLE

Page No.

iv

LIST OF SYMBOLS

$E(k)$	=	kinetic energy of turbulent motion
g	=	gravity
k	=	wave number
O_3	=	ozone
S_{max}	=	maximum vertical shear
$V_a, V_{(u,v)}$	=	horizontal velocity of the air
V_d	=	horizontal velocity of the dipoles
w	=	vertical velocity
z	=	vertical coordinate
α	=	a universal constant
ϵ	=	rate of energy dissipation
ρ	=	air density
λ	=	wavelength
μ	=	micron (10^{-6} meters)

I. Introduction

A survey of man's current knowledge of the atmosphere (below that sampled by satellites) would indicate that a linear increase in altitude is inversely proportional in a non-linear (logarithmatical) manner to his knowledge of the atmospheric processes.

There are many techniques, direct and indirect, for determining high altitude atmospheric parameters. The direct methods are several: (1) The standard global meteorological balloon launched radiosonde reaches heights > 30 km twice daily; (2) Grenades have been placed at high altitudes ($20 < z < 100$ km) at irregular intervals (see e. g., Nordberg and Stroud, 1961); (3) Meteorological rockets in the North American network now sample the upper atmosphere ($20 < z < 80$ km) on a quasi-regular basis (see e. g., Webb et al., 1961). Meteorological soundings are made at irregular intervals at heights greater than 80 km; (4) Certain U. S. Army large diameter, extended barrel guns are capable of placing a payload well above 100 km. The more practical use for these guns is that of placing chaff (or parachute) to altitudes of 70 to 80 km and tracking the chaff dipoles, as they descend (see e. g., Smith, 1960; McGill University, 1963; Williamson, 1966).

It suffices to mention only several of the indirect techniques in passing: (1) Radiometeor tracking (see e. g., Greenhow, 1952; Lovell, 1954; Greenhow and Neufeld, 1959) has been useful since the early 1950's to determine high altitude winds; (2) The determination of temperature and wind by the anomalous propagation of sound is another useful technique (see e. g., Crary and Bushnell, 1955). The use of the lidar, which uses a monocromatic pulse from a laser, has been helpful in locating aerosol layers at various altitudes (see e. g., Fiocco and Smullin, 1963).

This paper is concerned primarily with the determination of high-altitude winds as inferred from the movement of small volume chaff dipole "clouds". It is, therefore, useful to examine briefly

the first technique employed to place chaff dipoles at mesospheric heights.

As early as 1955 planning began to initiate high altitude measurements of wind by means of chaff dipoles (aufm Kampe, 1956; Anderson and Hoehne, 1956). In 1956 Anderson (1957) described a project that had placed chaff at 35 km by means of a Loki-type rocket. The chaff was successfully tracked by radar. A few months later Anderson (1957) reported successful tracking from an altitude of 46 km. Aufm Kampe (1957) reported in 1956 radar tracking of chaff at an altitude of 76 km. These chaff dipoles were placed at this height by means of a rocket launched from the White Sands Missile Range.

Two years after the first rocket placed chaff in the mesosphere a series of high-altitude chaff "bundles" were placed in the mesosphere by large diameter, extended barrel guns. These guns fired projectiles that provided a closely spaced time series of inferred winds (30 to 91 km) over Johnson Island and Tonopah, Nevada (Smith, 1960). The high-altitude gun probe sampling technique has been used at irregular intervals since 1959 (see e. g. , Murphy and Bull, 1968; Williamson, 1966; Williamson and Boyer, 1966).

In September 1969 a high-altitude gun probe project was initiated in the Colorado Rocky Mountains (Lovill, 1969; Reiter et al. , 1969; Reiter and Lovill, 1970). The purpose of the project was to determine small- and meso-scale atmospheric structure from the surface to the mid-mesosphere. This paper describes this experiment and its results.

II. Experimental Procedure

Geographical Location of the Gun Probe and Balloon Release Sites

The gun probe system and radar site 1 were located at Camp Hale, an abandoned Army high-altitude training base. Camp Hale (elevation: 2830 meters) is 9 km NW of Climax, Colorado. The radiosonde and ozonesonde release site and radar site 2 were located at the Chalk Mountain Observatory. The Observatory (elevation: 3658 meters) is 1 km WNW of Climax, Colorado (110 km SW of Denver).

Ozonesondes, radiosondes, constant level balloons, and surface ozone sensors were used to provide supplemental data from the mid-troposphere (observatory level) to the upper stratosphere. This supplemental data will be discussed at length in Appendices A, B, and C.

The High Altitude Gun Probe Experiment

The gun probe has several distinct advantages over the standard meteorological rocket: (1) The gun probe is considerably less expensive than the rocket. This factor alone allows many more probes of the upper atmosphere from a cost view-point; (2) The chaff payload can be accurately placed at a pre-selected location in the mesosphere. The advantage is obvious: The same location in the mesosphere can be sampled at regular intervals. The remarkable ability of the launch system to place chaff dipoles consistently at approximately the same location in space is borne out by the following. A comparison of chaff dipole locations a few seconds after expulsion at apogee (a data set acquired on 16 September at 0630 MDT, not included in the paper for reasons mentioned later, vs. a data set on 12 September at 0021 MDT) shows a separation near 69 km altitude of $x = 0.9$ km, $y = 2.7$ km, $z = 1.3$ km. These values may be considered typical. (3) The use of meteorological rockets is restricted to essentially unpopulated areas (e. g., White Sands Missile Range) because of the

large possible impact region. In the lower atmosphere the projectile is less susceptible to extreme environmental conditions due to its high velocity. The gun probe impact area is well-defined and much smaller than that of the rocket. It is for this reason that the gun projectile is a safer research tool for use in a sparsely populated region such as the Colorado Rockies. There were two impact areas, each 3 x 16 kilometers, for the two guns at Camp Hale. One gun was fired to the north, the other to the south.

Equipment

The two guns at Camp Hale had a barrel length of 13.4 meters. The smooth-bore of the gun was 13.7 cm in diameter.

The probe was a HARP 5.1 projectile. It has a length of 1.14 m and a weight of approximately 10 kilograms (Williamson, 1966). The aluminum dipoles are 25μ in diameter; the copper dipoles 125μ. Only the behavior of the aluminum chaff will be discussed in this paper. At the present time the projectile is used principally with chaff. Tests are being conducted with thermistor units that could be released at apogee. The restriction to use of chaff-type targets only is a result of the extremely large acceleration of the projectile in the barrel, equal to approximately 60,000 g.

The radars at Camp Hale and at the Observatory simultaneously tracked the chaff dipoles upon release at a preselected apogee.

III. Evaluation of Parameters

The rate of fall of the 25μ chaff is much slower than that of the 125μ chaff. The fall rate of the 25μ chaff is given by a best fit curve through the observed mean fall rates for individual probes (see Figure 1). Whereas the 125μ chaff is used to determine wind velocities over large vertical distances, the 25μ chaff is more indicative of horizontal motions. The heavier chaff can fall from 70 to 40 km in 20 minutes. The 25μ chaff will fall less than 7 km in the same period. An example of the relatively slow fall rate of the 25μ chaff is seen in Figure 2 which indicates a fall rate of approximately 4 km in 20 minutes. Also note that there is very little height change from minute 13 to 20. Large upward motions seem to be in evidence during the last one-third of the tracking.

Error Analyses

Studies have been conducted by Smith (1960) and Rapp (1960) on possible errors resulting from radar tracking of high altitude chaff. The reader is invited to refer to their error analyses for in-depth discussion. The primary errors in determining the actual wind in the stratosphere and mesosphere from chaff observations follow.

Dipole Diffusion. Approximately 10^6 dipoles are ejected from the projectile at apogee. Smith (1960) has observed the fall characteristics of large numbers of chaff dipoles in ambient conditions near the ground and states that they fall like a sheet of paper. A few seconds after expulsion of the chaff at high altitudes the chaff "cloud" is small in volume and provides a strong discrete reflection. In time the dipoles diffuse outward from their common center-of-gravity and provide a weaker signal. With increasing time the chaff may separate into several clusters. As long as the radar tracks a single cluster, the track will be a good one. But if there are several clusters of equal reflectivity, and since the radar automatically tracks the
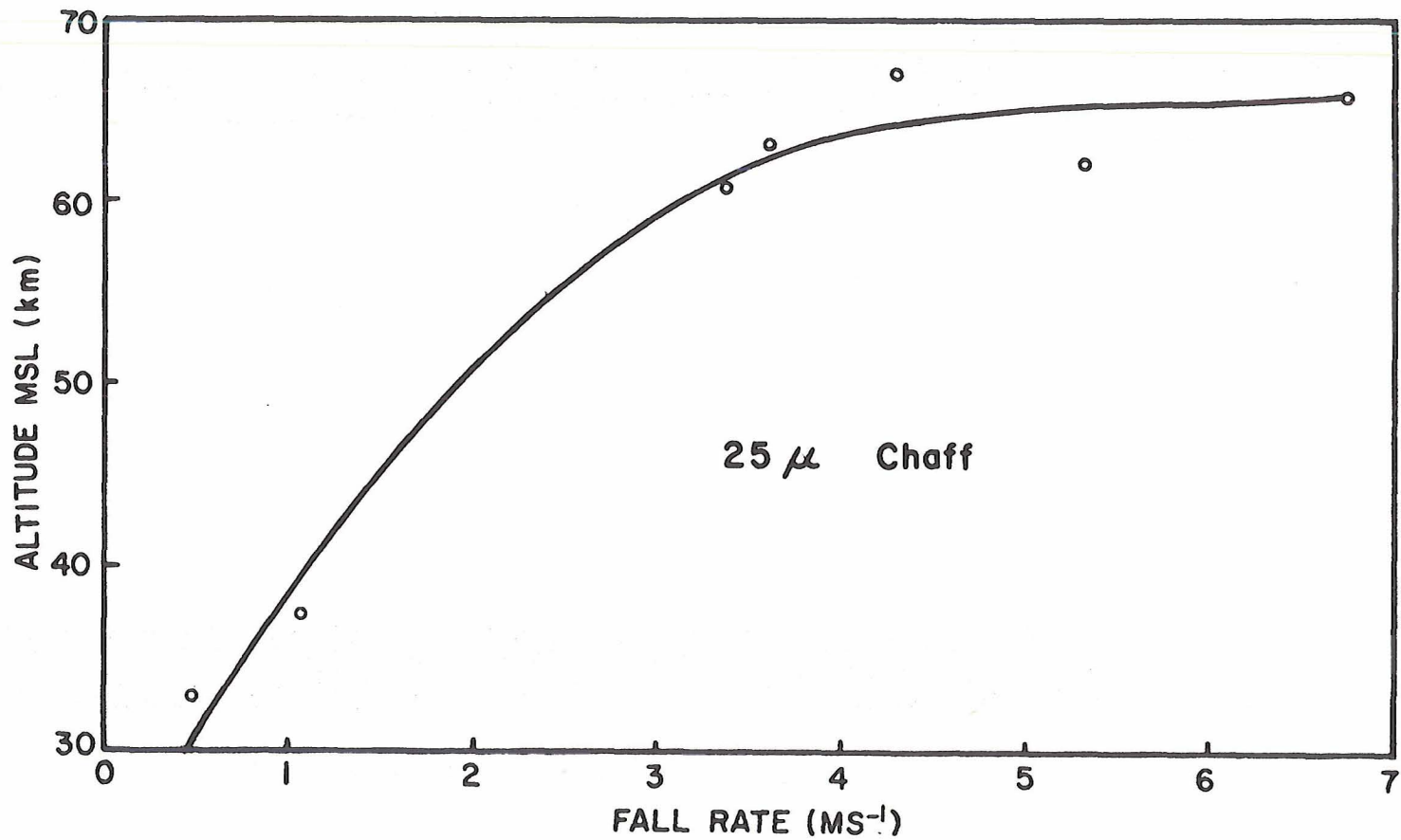
Figure 1. The fall rate of 25μ chaff at various altitudes as observed during the September 1969 project. Each circle represents the mean fall rate of the chaff of one high-altitude sounding.

CHAFF   25 SEPT 69   06:00 MDT
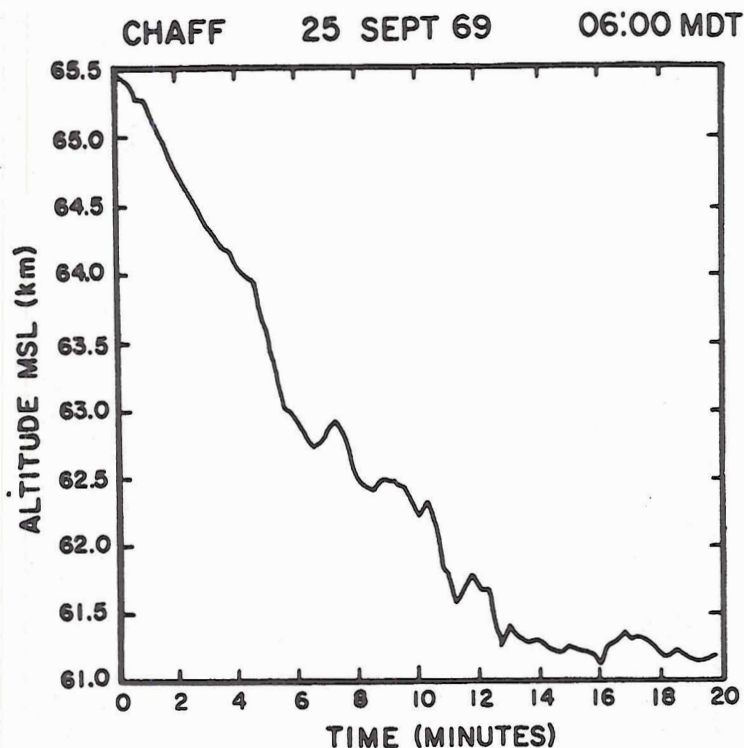
Figure 2. Smoothed location of chaff target
with time.

strongest signal, the tracking may become erratic as the radar

switches from one target to another. The latter appeared to be

the case for one chaff data set. These data are not included in

this study.

Although Smith (1960) reports an automatic track of 52 min-

utes length of high-altitude chaff, there is little doubt that the last

part of the data gathering period did not provide data on atmospheric

wind variation as good as did the first part. Chaff targets were tracked

for as long as 35 minutes during September 1969; however, the only

data presented in this report was terminated at expulsion plus 15 to

20 minutes.

By keeping the data period short and by elimination of data that

appeared influenced by random variations of reflectivity within the

chaff cloud, we have kept the diffusion problem to a minimum.

Data Reduction. Some errors will, of course, occur during data reduction. It is felt, however, that these errors will be both small and random and therefore insignificant when compared to the previous possible errors.

The Relation Between Chaff Motion and Actual Air Motion. It is necessary to know the response of chaff to air motions. Because the chaff dipole has a certain mass, its motion and that of the air do not have a one-to-one relation. Fluid resistance controls the response of the chaff to various wind components as it falls toward the earth's surface under the influence of gravity. Rapp (1960) gives an equation by which the difference between the horizontal velocity of the dipoles (V_d) and the horizontal velocity of the air (V_a) is found.

$$V_d - V_a = - \frac{w^2}{g} \frac{dV_d}{dz} \, ,$$

where w = the rate of fall of the dipoles at a given height, z,

g = gravity,

and $\dfrac{dV_d}{dz}$ = is the mean velocity change of the dipoles through the region under study.

To gain insight into the response of the dipoles to atmospheric motions a typical case is presented. At 0600 MDT on 25 September the mean rate-of-fall (w) of the dipoles from 62.5 to 61.5 km was 4 m s^{-1}, $dV_d/dz = 4 \text{ m s}^{-1} \text{ km}^{-1} = 4 \times 10^{-3} \text{ s}^{-1}$. The value of g at 62 km = 9.62 m s^{-2}. This gives a $V_d - V_a = 1.3 \times 10^{-2} \text{ m s}^{-1}$.

The maximum value of $V_d - V_a$ for all of the data sets discussed was $2 \times 10^{-1} \text{ m s}^{-1}$ (w = 8 m s^{-1}, $dV_d/dz = 3.5 \times 10^{-2} \text{ s}^{-1}$, z = 67 km).

It, therefore, is obvious that the typical value of $V_d - V_a$ is $\ll 1 \text{ m s}^{-1}$. Even the maximum difference between V_d and V_a is $< 1 \text{ m s}^{-1}$. Since the computed corrections are one to two orders of magnitude less than the normally encountered velocities in the

mesosphere during this study, the corrections will be neglected in the computation of all velocities.

Fall Reversal of Stratospheric and Mesospheric Wind

During July and early August over North America easterly winds reach their maximum velocity in the stratosphere and lower mesosphere. In general in mid-latitudes these winds decrease considerably by September. Shortly thereafter the wind once again increases in velocity and is now from the west. This appears to be a direct influence of the decreasing solar angle in the Northern Hemisphere (see e. g., Miers, 1963; Webb, 1966). The reversal seems to be centered about the autumnal equinox.

Wind vectors at 13 levels from 13 to 34 km were averaged for the months of July-November, 1959-1968 inclusive for Denver, Colorado (Lovill, 1969). It was observed that wind velocities are stronger at 13-20 km during October and November than July and August (Figure 3). From 20-34 km the easterlies during July and August are ~ 1.5 times as strong as the westerly flow in October and November. A change from high altitude zonal easterly flow to westerly flow was observed to occur during September. During this transition month, velocities at all levels above 17 km are small. The data in this paper were collected between 12 and 27 September. This period coincided with the autumnal equinox.

Figure 4 represents six of the stratospheric and mesospheric chaff inferred wind profiles plotted at 0.5 km increments; therefore the fine structure is not seen in this figure. The two lower profiles at 33 and 37 km are shown only to indicate that the flow at these levels was weak and from the east. More variability is seen in the mesosphere. If we attempt to determine whether the easterlies have decreased, or indeed become westerlies, at a particular level during the period from the middle to the end of September, a general trend can be seen. There are four soundings
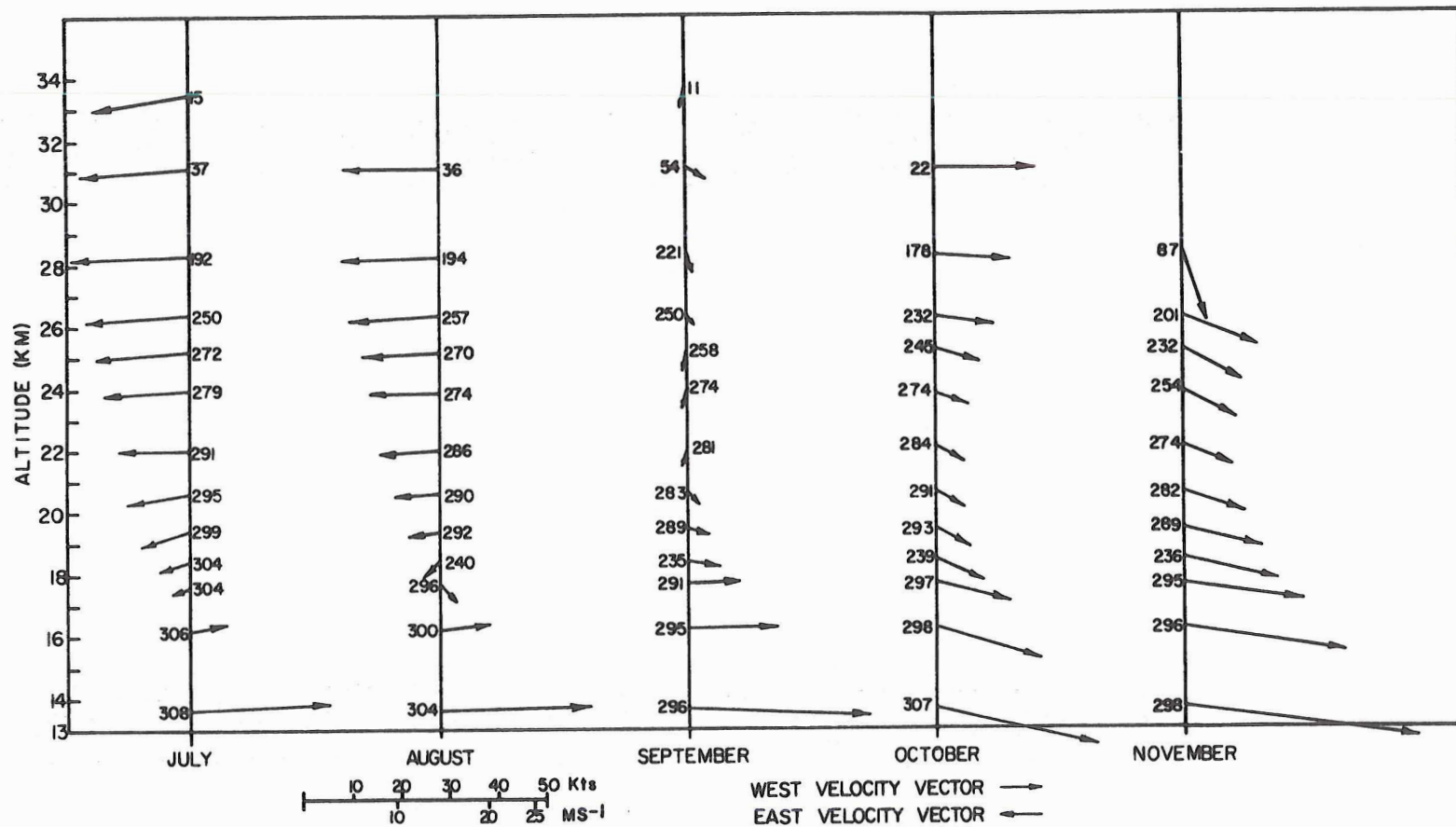
Figure 3. Horizontal velocity vectors at levels between 13 and 34 km for July-November for ten years of data at Denver, Colorado. (The number next to the velocity vector indicates the number of observations used to compute that particular vector.)
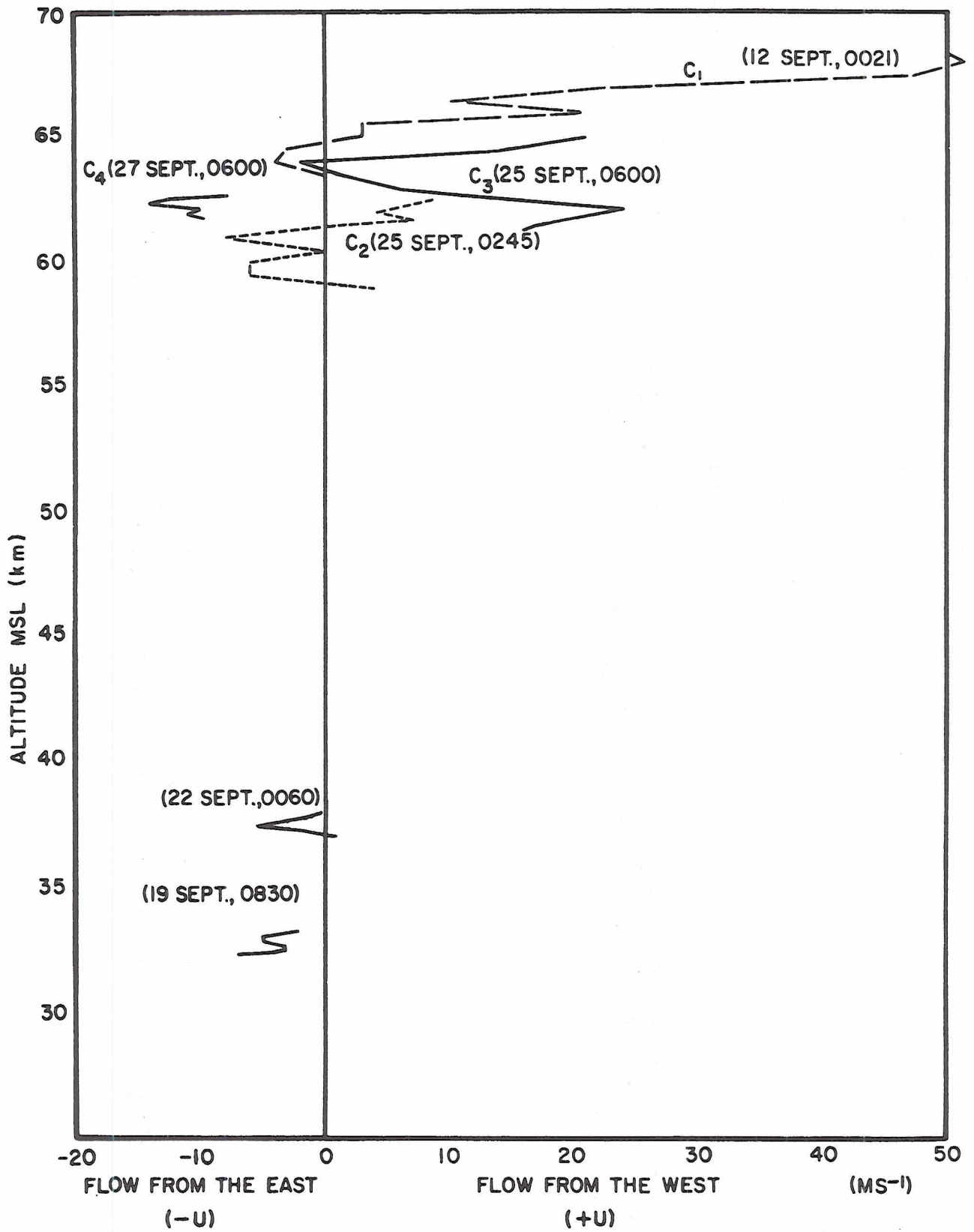
Figure 4. Profiles of the u-component in the stratosphere and meso-
sphere for six chaff soundings.

at approximately 63 km. The 12 September sounding (c_1) indicates a calm condition at this level. The data on 25 September at 0300 MDT (c_2) show a velocity of 8 m s^{-1} from the west. The sounding three hours later (c_3) indicates approximately the same velocity and direction. The 27 September sounding (c_4) three days later shows a velocity of approximately 8 m s^{-1}, but from the east. At this 63 km level, there appears to be no evidence of a reversal. However, it is possible that the reversal has already occurred and what we are seeing are simply remnants of the easterlies represented by thin layers interspersed among thick layers of the dominant westerly flow. It appears as if the change in wind direction is at best described as irregular during this sampling interval in the mesosphere.

An interesting feature to note is the 51 m s^{-1} u-component of the wind in the c_1 profile at 68 km. The flow at this level is strongly zonal. The meridional component is only 2 m s^{-1}.

Detailed Examination of Mesospheric Data

Horizontal Velocity and Vertical Shear. Table 1 lists pertinent data relative to the four data sets analyzed. All maximum velocities were > 25 m s^{-1} and all but c_4 had a westerly component. Minimum velocities were small as anticipated during this period. The maximum shear encountered was 35 m s^{-1} km^{-1} as seen in data set c_1. All shears were computed by analyzing one kilometer increments. The vertical profile of the $V_{(u, v)}$ for data set c_1 is given in Figure 5. Also note the shear of approximately 43 m s^{-1} in the layer from 68.1 to 66.4 km.

The $V_{(u, v)}$ maxima for both 25 September chaff data sets (c_2, c_3) occur at exactly the same height (62.2 km) and at approximately the same $V_{(u, v)}$ (26 and 28 m s^{-1}, respectively).

Table 1: Mesosphere Chaff Dipole Data

Data Set No.	Date (Sept)	Time of Acquisition (MDT)	Altitude chaff tracked (km) From	To	Mean W $(m\,s^{-1})$	Max W $(m\,s^{-1})$	Direction (from)	Min W $(m\,s^{-1})$	S_{max} $(m\,s^{-1}km^{-1})$	Mean altitude of $S_{max}(km)$
c_1	12	0021	68.7	63.7	27.0	52.7	275	3.5	35.0	67.0
c_2	25	0245	62.5	58.9	12.5	26.0	330	4.5	26.0	61.9
c_3	25	0600	65.4	61.1	18.5	28.0	295	7.5	15.4	64.5
c_4	27	0600	62.7	61.8	20.5	25.3	020	14.5	15.5	61.2

S_m = maximum vertical shear

W = two-dimensional horizontal wind

-13-

CHAFF   12 SEPT 69   00:21 MDT
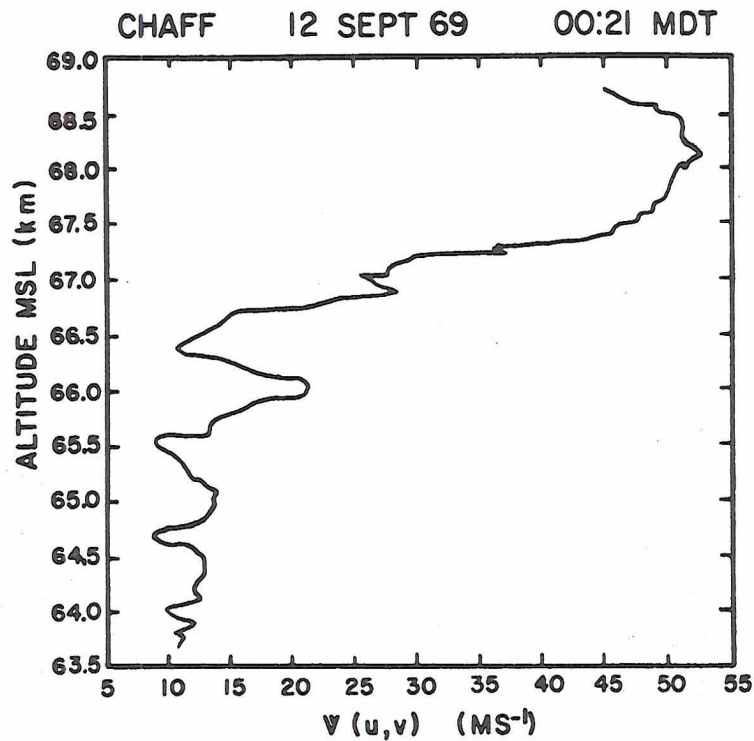
Figure 5. Vertical profile of the horizontal wind (data set c_1) in the mesosphere.

Vertical Velocity. Vertical velocity of the air (w_a) was computed by performing a three-minute running mean of the chaff rate-of-fall and subtracting the instantaneous rate-of-fall.

The maximum + w_a (directed upward) for all data sets was + 7.5 m s^{-1} in c_1. This occurred in a region centered on 64.2 km over a time interval of two minutes. Maxima (+ w_a) for c_2, c_3 and c_4 were 0.9, 6.5 and 4.5 m s^{-1}, respectively. These upward directed velocities occurred at heights ranging from 61.3 to 63.9 km. Velocity of similar magnitude was found for -w_a for all data sets.

One data set (c_3) should be given special attention. Figure 2 depicts the location of the chaff cloud at various times. Particular notice should be given the last seven minutes of data. From minute 12.8 to 19.8 the chaff cloud fell approximately 100 meters. The

average rate-of-fall at 61250 meters (see Figure 1) is $3.3 \, \text{m s}^{-1}$.
This means that the average $+ w_a$ for this seven-minute period was
$+ 3.1 \, \text{m s}^{-1}$.

It appears as if significant vertical motion, both upward and downward, occurred during all chaff dipole descents. The analysis in c_3 indicates a particularly prolonged upward motion. The most likely explanation of these phenomena is that gravity wave (either stationary or traveling) activity is responsible. Many authors (see e.g., Hines, 1960) have given theoretical evidence of gravity waves at these altitudes. Assuming that these vertical motions are gravity wave produced, it is difficult to determine whether they are the result of orographic barriers or whether some other cause is responsible for their formation.

IV. A Spectral Analysis of Chaff Velocity Components
in the Mesosphere

The structure of the mesosphere is directed toward instability with respect to convective activity. It is a region in which quite large vertical wind shears can exist. Indeed, in the region investigated (60 to 70 kilometers) shears of 35 $m\,s^{-1}\,km^{-1}$ were measured. (Aufm Kampe et al. (1962) during Project Shotput studied a region between 60 and 110 km. They reported a shear of 100 $m\,s^{-1}\,km^{-1}$.)

Past measurements (see e. g. , Shur, 1962; Vinnichenko et al. , 1965; Reiter and Burns, 1966; Pinus et al. , 1967) have indicated the presence of distinct regions of energy input at discrete wavelengths. The above measurements suggest energy input appears to occur at several wavelengths, the shorter wavelengths being less than approximately 60 km which corresponds to phenomena at the small- to meso-scale range, possibly produced by lee waves. Energy input also appears at wavelengths of approximately one kilometer. This apparently corresponds in our case to short gravity-shearing waves found in the mesosphere.

The wind field measured from the chaff motion in the present study indicates motions other than those of simple zonal and meri-dional atmospheric flow in the mesosphere. Wave motions (discussed above) appear to be reflected in our data. This investigation was conducted in the Rocky Mountains, therefore it is quite possible that flows at mesospheric heights to some extent reflect orographic features below. It is these features that we look to for energy input at the mesoscale.

Additionally at certain critical wavelengths a large amount of turbulent energy is made available to the flow through the vertical shearing stresses. These stresses will bring about Kelvin-Helmholtz type instabilities in the flow even though thermal stability existed. A region of instability, due to these gravitational shearing waves, will exist if

$$\Delta\rho \; - \; \frac{k\bar{\rho}}{2\,g}\,(\Delta\bar{u})^2 < 0 \qquad\qquad \text{(Reiter, 1963)}$$

$\Delta\rho$ is the density change, k the wave number, and $\Delta\bar{u}$ the wind shear.

The high frequency turbulence data to be presented later is at wavelengths at which the inertial subrange of Kolmogoroff's similarity hypothesis should apply. Kolmogoroff's hypothesis (Kolmogoroff, 1941) states that energy is put into a system in large eddies and extracted by viscous dissipation in smaller eddies. The inertial subrange exists within eddy sizes between the above eddy sizes. Turbulence in the inertial subrange is of an isotropic nature. Power spectra in the inertial subrange are represented by the -5/3 law.

Batchelor (1959) has shown that the energy spectra of turbulence in the inertial subrange may be written as follows

$$E(k) = \alpha\,\epsilon^{2/3} k^{-5/3}$$

E(k) is the kinetic energy (K. E.) of turbulent motion in the wave number range k to k + dk, α is a universal constant, and ϵ is the rate of energy dissipation.

Various authors have attempted to assign upper and lower limits to the inertial subrange. These estimates vary from a lower limit estimate of several centimeters to an upper limit estimate of approximately 600 meters. Batchelor (1950) suggested that the upper limit had to be at least 100 meters. MacCready (1962) has suggested an upper limit of approximately 300 meters. Shur (1962) and Pinus et al. (1967) have suggested that the upper limit may be as great as 600 meters. Much of the data in this investigation is in the 300 to 600 meter wavelength region so the inertial subrange and its inferences of isotropy are of importance in this study. Additionally effects on aircraft imply that much energy is in the 300 to 600 meter wavelength range (see e. g., MacCready, 1962).

At wavelengths greater than 600 meters (Shur, 1962) the so-called buoyant subrange may exist under conditions of stable stratification (see e. g. , Bolgiano, 1959; Monin, 1962; Lumley, 1965; Reiter, 1966; Pinus et al. , 1967). It has been proposed that the buoyant subrange may also exist under conditions of stable stratification with scale lengths from as low as 30-100 meters up to scales where energy production is balanced by damping due to the buoyant forces (Pinus et al. , 1967).

Data Interpretation

Three sets of data each of 1080 seconds duration at the 60-70 kilometer height interval were analyzed. The data were prepared for analysis by first performing a trend removal. Next a low pass filter was used on the data. This consisted of applying the following smoothing technique

$$(j_{-1} + 2j + j_{+1}) / 4$$

where j is the point to be smoothed and j_{-1} and j_{+1} are points in time before and after j. The standard Blackman and Tukey (1958) method was applied to each component of each data set to obtain independently the power spectral densities.

The three sets of data were obtained from chaff releases on 12 and 25 September 1969 in the mesosphere over the Colorado Rockies. One data set was obtained beginning at 0021 MDT on 12 September--designated data set 1; a second data set at 0245 MDT, 25 September--data set 2; and a third 3. 3 hours later, at 0600 MDT--data set 3.

Data Set 1

Figure 6 represents the spectral analysis of the u-, v-, and w-components of data set 1. The spectral density curves have been normalized. A note of caution in the interpretation of the high frequency end of the spectra--because of the method of computing the power spectral densities, aliasing problems may be suspected. Although the following plots of energy spectra may extend to high frequencies, interpretation is not given at frequencies greater than $1/35$ sec^{-1}.

Overall, the u-, v-, and w-components have an average spectrum slope of approximately -5/3 in the doubly logarithmic plots. The u- and v-spectra slopes are almost exactly the same at wavelengths less than 2.7 km. At lower frequencies u-spectra appear to have more energy available. The spectral curves suggest a significant difference in the K. E. of the w- and u-spectra at the frequency $1/35$ sec^{-1}. This anisotropy is quite large even if the spectra are normalized.

A spectral peak is seen at $1/35$ sec^{-1} on all three component spectra. The w-spectra peak is, however, a good deal stronger. A spectral gap is seen in the w-spectra at about $1/50$ sec^{-1}. A smaller gap is seen in the u- and v-spectra at $1/40$ sec^{-1}. A spectral gap such as this could be indicative of turbulent energy decaying more rapidly than by a breaking-up of large eddies into smaller eddies. At wavelengths greater than 1.2 km the u- and v-spectra suggest an energy supply acting rather continuous.

Data Set 2

The average slope for the u- and v-spectra (Figure 7) is approximately -13/5 over the entire spectrum ($1/35$ to $1/350$ sec^{-1}, which corresponds to a wavelength from 300 to 6000 meters). The w-spectra have a less steep slope, -11/5. At increasing frequencies the spectral slope of all three parameters increases slightly.
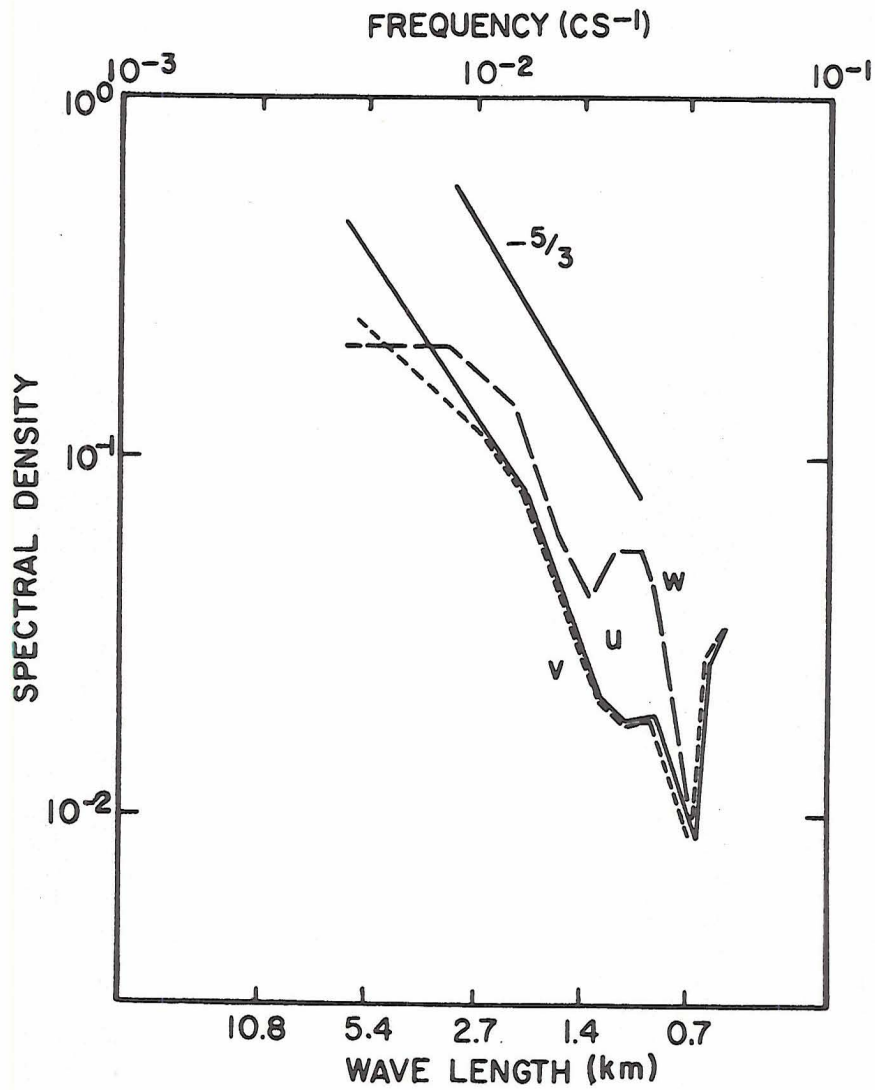
Figure 6. Normalized spectral density of the u-, v-, and
w-components of the chaff track beginning at 68.7 km
altitude at 0021 MDT on 12 September 1969 (ordinate
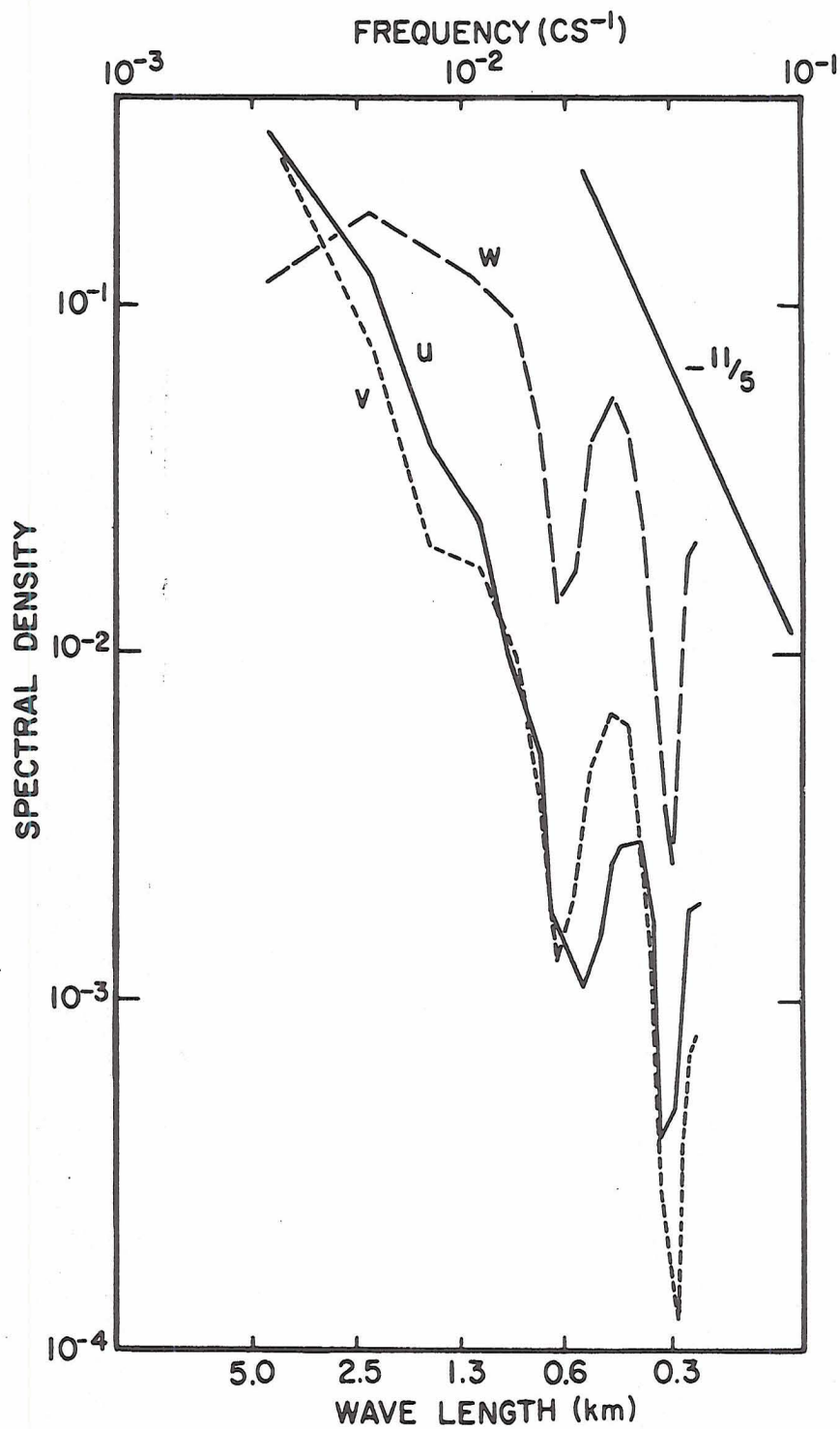in terms of $n F(n)/nf(n)_{max}$). See text for elaboration.

Figure 7. Normalized spectral density of the u-, v- and w-components of the chaff track beginning at 62.5 km altitude at 0245 MDT on 25 September 1969. See text for elaboration.

Several interesting features are immediately obvious when the various spectra are compared in Figure 7. Firstly, there appears to be quite a bit more energy in the w-spectra than the u- or v-spectra at high frequencies. Secondly, there is a reversal of this trend at a frequency of $1/250$ sec^{-1}. Therefore at the lower frequencies (longer wavelengths) there is less energy available in the w-spectra than either the u- or v-spectra. Thirdly, significant K. E. appears in the w-spectra at about $1/200$ sec^{-1} (a wavelength of 2400 m). This does not appear in either the u- or v- spectra. The spectra are rather continuous at these wavelengths.

A very strong spectral peak occurs at approximately $1/35$ sec^{-1} (400 m) on all component spectra. Since a spectral peak occurs at approximately $1/35$ sec^{-1} in all three data sets, there is a possibility that the peak may have been produced by the tracking equipment ("hunting" through the chaff cloud). A rather strong spectral gap appears in all three spectra at about $1/50$ sec^{-1}.

A comparison of the energy of the non-normalized spectra (not shown) indicates the following K. E. ratios: Throughout the high frequency end of the spectrum (frequencies higher than $1/60$ sec^{-1}) the ratio of K. E. in the u-, v-, and w-spectra is approximately 1:4:10. At frequencies from $1/60$ sec^{-1} to $1/160$ sec^{-1} the K. E. ratio is approximately 1:2:1. At the lowest frequency (~ 6000 m) this ratio becomes 2:7:1.

Data Set 3

The spectral slopes in Figure 8 are very similar to those in Figure 7. (It should be kept in mind that data sets 2 and 3 are separated in time by only three hours.) Near the low frequency end of the spectrum ($1/80$ to $1/350$ sec^{-1}, equivalent to approximately 1600 to 6000 m) the u- and v-spectra approach a -5/3 slope. The w-spectra is closer to a -2 slope. However at the higher frequencies the u-, v-, and w-spectra are approximated by a -11/5 slope.
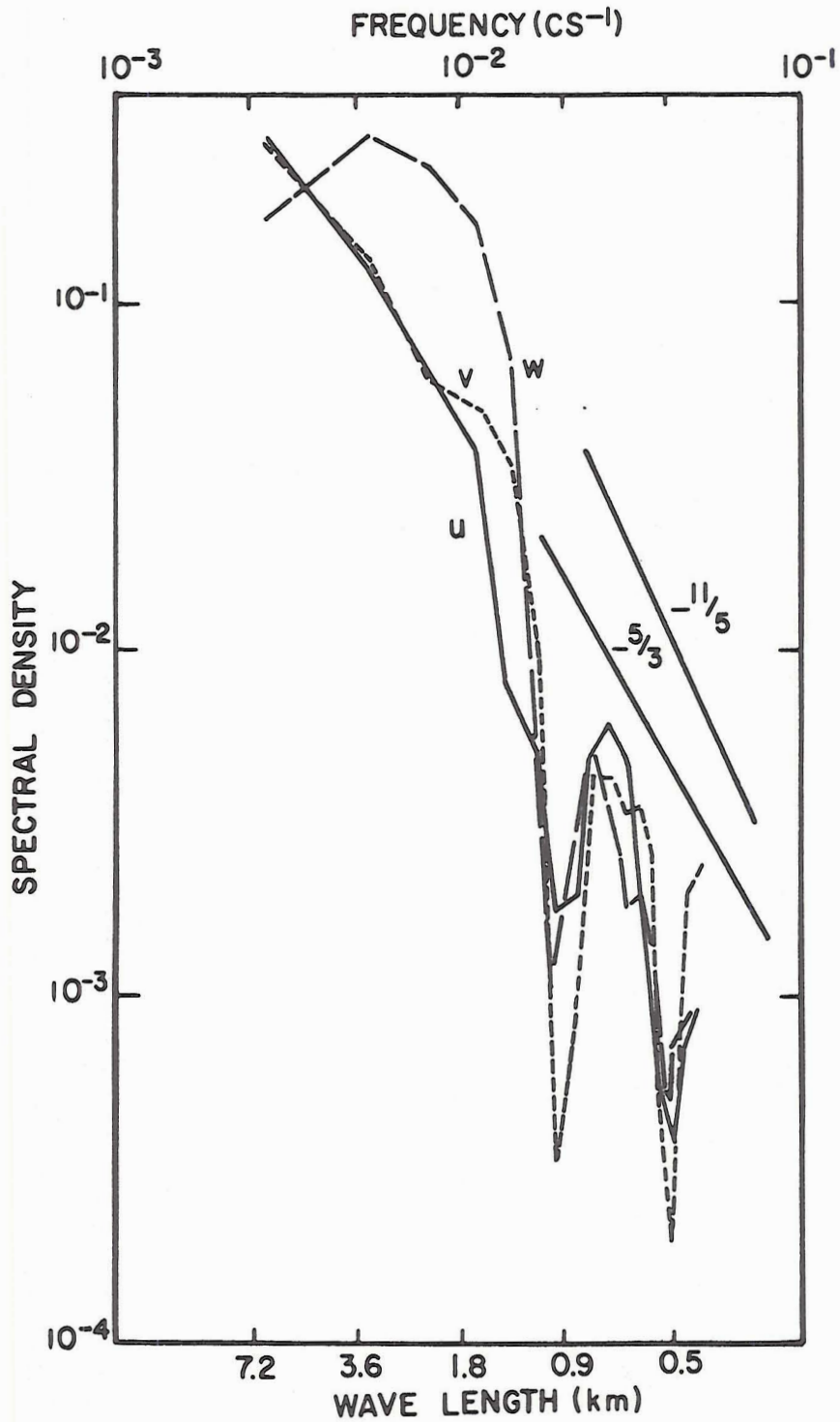
Figure 8. Normalized spectral density of u-, v- and w-
components of the chaff track beginning at 65.4 km
altitude at 0600 MDT on 25 September 1969. See
text for elaboration.

A dominate peak is seen in the w-spectra at $1/180$ sec^{-1} (λ = 3500 m). However, no such indication is reflected in the u- or v-spectra plot.

A strong peak is seen at $1/35$ sec (λ = 600 m) in all three spectra components. An equally strong gap is measured at $1/50$ sec (λ = 750 m) in all spectral components. A strong gap is also indicated at $1/25$ sec^{-1}, but as mentioned earlier, this frequency is too near the Nyquist frequency (the highest frequency which can be determined in a Fourier analysis of a discrete sampling of data) of the spectral analysis to be considered important.

Data set 2 experienced a maximum shear (S_m) of 26 m s^{-1} km^{-1}. Data set 3, however, experienced a S_m of half this magnitude. The ratio of the non-normalized energy spectra of w in set 2 to that of set 3 is E_{w_2} / E_{w_3} = 6. This suggests that the shear affects strongly the kinetic energy of the vertical component of motion.

V. Summary

A series of high-altitude gun probes was launched during September 1969 near Climax, Colorado. Chaff dipoles (25μ diameter) were ejected from the probe and tracked from 70 to 60 kilometers altitude.

An error analysis indicated that the greatest single uncertainty in data interpretation could result from dipole diffusion. This problem was minimized by using only data that were obtained in the early stage of the dipole tracking, when the diffusion was small.

An analysis was performed to determine to what extent the chaff motion reflected the actual motion of the air. It was determined that the response of the chaff was quite good under the normal vertical shear conditions encountered in the mesosphere.

The project was conducted during September in order to learn more of mesospheric flow conditions occurring during the fall reversal of wind. It appeared as though westerly winds were already evident at most levels from 60 to 70 kilometers by the time the project began (mid-September). There was also a suggestion that the reversal, instead of progressing steadily downward in time, might have occurred in thin layers. This was based on the fact that some easterly flow was still embedded in the basic westerly flow late in September.

A maximum velocity of 53 m s^{-1} and a maximum shear of 35 m s^{-1} km^{-1} were observed. Positive vertical motions of 8 m s^{-1} and negative motions of 9 m s^{-1} were recorded. A positive vertical motion of 3 m s^{-1} was recorded during seven minutes of data collection at a mean height of 61 kilometers. This appeared to be direct evidence that gravity wave motion was observed.

Power spectra of the u-, v- and w-components of various data sets were analyzed to give insight into the frequency distribution of spectral peaks and gaps at relatively short wavelength ($\lambda < 6000$ m).

Spectra gaps and peaks were observed to occur at similar wave numbers for different data sets. Turbulence at $\lambda < 600$ meters appeared to be isotropic in nature. In two data sets (~ 3 hours separated in time) it appeared that significant u- and v-component shears in the vertical in the first data set resulted in much greater K. E. in the w-spectra than in the later set which exhibited much smaller shears.

VI. Acknowledgements

VII. References

Aldaz, L., Flux measurements of atmospheric ozone over land and water. J. Geophys. Res., 74, pp. 6943-6946, 1969.

Anderson, A. D., Comments on upper air wind measurements with small rockets. J. Meteor., 14, pp. 473-474, 1957.

_____, and W. E. Hoehne, Experiments using window to measure high-altitude wind. Bull. Amer. Meteor. Soc., 37, p. 454, 1956.

aufm Kampe, H. J., Upper air wind measurements with small rockets. J. Meteor., 13, pp. 601-602, 1956.

_____, Reply to A. D. Anderson's, "Comments on upper air wind measurements with small rockets". J. Meteor., 14, p. 474, 1957.

_____, M. E. Smith, and R. M. Brown, Winds between 60 and 110 kilometers. J. Geophys. Res., 67, pp. 4243-4257, 1962.

Batchelor, G. K., The application of the similarity theory of turbulence to atmospheric diffusion. Q. J. Roy. Meteor. Soc., 76, pp. 133-146, 1950.

_____, The Theory of Homogeneous Turbulence. Cambridge University Press, 197 pp., 1959.

Blackman, R. B., and J. W. Tukey, The Measurement of Power Spectra from the Point of View of Communications Engineering. Dover Publications, New York, 190 pp., 1958.

Bojkov, R. D., Planetary features of total and vertical ozone distribution during IQSY. NCAR Manuscript Number 430, 113 pp., 1967.

Bolgiano, R., Jr., Turbulent spectra in a stably stratified atmosphere. J. Geophys. Res., 64, p. 226, 1959.

Crary, A. P., and V. C. Bushnell, Determination of high-altitude winds and temperatures in the Rocky Mountain area by acoustic soundings, October 1951. J. Meteor., 12, pp. 463-471, 1955.

Dütsch, H. U., Photochemische Theorie des atmospharischen Ozons unter Beruchsichtigung von Nichtgleichgewichtszustanden und Luftbewegungen. Ph. D. Thesis, University of Zurich, Switzerland, 1946.

Fiocco, G., and L. D. Smullin, Detection of scattering layers in the upper atmosphere (60-140 km) by optical radar. Nature, 199, p. 1275, 1963.

Greenhow, J. S., A radio echo method for the investigation of the atmospheric wind at altitudes of 80 to 100 km. J. Atm. Terr. Phys., 2, p. 282, 1952.

_____, and E. L. Neufeld, Turbulence at altitudes of 80-100 km and its effect on long-duration meteor echoes. J. Atm. Terr. Phys., 16, p. 382, 1959.

Hering, W. S., and T. R. Borden, Jr., Ozonesonde observations over North America, Vol. 4. A. F. Cambridge Res. Lab., AFCRL-64-30(IV), Environ. Res. Papers No. 279, 1967.

Hines, C. O., Internal atmospheric gravity waves at ionospheric heights. Canadian J. Physics, 38, pp. 1441-1481, 1960.

Junge, C. E., Air Chemistry and Radioactivity. Academic Press, New York and London, 382 pp., 1963.

Kolmogorov, A. N., The local structure of turbulence in incompressible viscous fluid for very large Reynolds numbers. Comptes Rendus (Doklady), Acad. Sci., U. R. S. S., 30, pp. 301-305, 1941.

Komhyr, W. D., Electrochemical concentration cells for gas analysis. Ann. Geophys., 25, pp. 203-210, 1969.

Kroening, J. L., and E. P. Ney, Atmospheric ozone. J. Geophys. Res., 67, pp. 1867-1875, 1962.

Lovell, A. C. B., Meteor Astronomy. Oxford University Press (Clarendon), London and New York, 464 pp., 1954.

Lovill, J. E., The vertical distribution of ozone and atmospheric transport processes over the San Francisco Bay area. Presented at the 48th Annual Meeting of the Amer. Meteor. Soc., San Francisco, California, 29 January - 1 February 1968.

_____, Transport processes in orographically induced gravity waves as indicated by atmospheric ozone. Atmos. Sci. Paper No. 135, Department Atmospheric Science, Colorado State University, 1969.

Lovill, J. E. , An abrupt change in the stratocpheric circulation dur-
ing September over Denver, Colorado: based upon ten years of
high altitude wind data.   Report No. 1 (Department of Atmos-
pheric Science to Atmospheric Sciences Offices, White Sands
Missile Range (U. S. Army DAAG 05-69-C-0866)), August 1969.

_____, Gravity wave measurements as simultaneously deter-
mined by satellite, ozone and airplane.   Arch. Met. Geoph.
Biokl., A, 19, pp. 13-28, 1970.

_____, and A. Miller, The vertical distribution of ozone over
the San Francisco Bay area.   J. Geophys. Res. , 73, pp. 5073-
5079, 1968.

Lumley, J. L. , The inertial subrange in non-equilibrium turbulence.
Paper given at the International Colloquium on the Fine-Scale
Structure of the Atmosphere, Moscow, June 15-22 1965.

MacCready, P. B. , Jr. , The inertial subrange of atmospheric turbu-
lence.   J. Geophys. Res. , 67, pp. 1051-1059, 1962.

McGill University, Project HARP, Report on the first twelve firings
and status as of 30 July 1963.   Department of Mechanical
Engineering, Report 63-5, 1963.

Miers, B. T. , Zonal wind reversal between 30 and 80 km over the
southwestern United States.   J. Atmos. Sci. , 20, pp. 87-93,
1963.

Monin, E. A. , On turbulence spectrum in temperature-inhomogeneous
atmosphere.   Izv. AN USSR, Geophys. Ser. , 3, 1962.

Murphy, C. H. , and G. V. Bull, Ionospheric winds over Yuma, Arizona,
measured by gun-launched projectiles.   J. Geophys. Res. , 73,
pp. 3005-3015, 1968.

Nordberg, W. , and W. G. Stroud, Results of IGY rocket-grenade
experiments to measure temperatures and winds above the
Island of Guam.   J. Geophys. Res. , 66, pp. 455-464, 1961.

Paetzold, H. K. , New experimental and theoretical investigations
on the atmospheric ozone layer.   J. Atmos. Terr. Phys. , 7,
pp. 128-140, 1955.

Pinus, N. Z. , E. R. Reiter, G. N. Shur, and N. K. Vinnichenko,
Power spectra of turbulence in the free atmosphere.   Tellus,
XIX, pp. 206-213, 1967.

Rapp, R. R. , The accuracy of winds derived by the radar tracking of chaff at high altitudes. J. Meteor. , 17, pp. 507-514, 1960.

Regener, V. H. , and L. Aldaz, Turbulent transport near the ground as determined from measurements of the ozone flux and the ozone gradient. J. Geophys. Res. , 74, pp. 6935-6942, 1969.

Reiter, E. R. , Jet Stream Meteorology. University of Chicago Press, Chicago and London, 515 pp. , 1963.

_____, Clear air turbulence: Problems and solutions (a state-of-the-art report). 1966 ION-SAE Clear Air Turbulence Conference, 9 pp. , 1966.

_____, and A. Burns, The structure of clear air turbulence derived from "TOPCAT" aircraft measurements. J. Atmos. Sci. , 23, pp. 206-212, 1966.

_____, and J. E. Lovill, The mesostructure of the atmosphere from the troposphere to the lower mesosphere over mountain-our terrain (A summary of activities during the September 1969 field project phase), Report No. 2 (Department of Atmospheric Science to Atmospheric Sciences Office, White Sands Missile Range (U. S. Army DAAG 05-69-C-0866)), January 1970.

_____, J. E. Lovill, and E. L. Williamson, Mesospheric and stratospheric wind structure over the Rocky Mountains, as deduced from gun probes and balloon-borne transponders. Presented at the American Geophysical Union Meeting, San Francisco, 15-18 December 1969.

Shur, G. N. , Experimental investigations of the energy spectrum of atmospheric turbulence. Tsentral'naya aerologischeskaya observatoriya. Trudy, No. 43, pp. 79-90, 1962.

Smith, L. B. , The measurement of winds between 100,000 and 300,000 ft by use of chaff rockets. J. Meteor. , 17, pp. 296-310, 1960.

Vinnichenko, N. K. , N. Z. Pinus, and G. N. Shur, Some results of the experimental turbulence investigations in the troposphere. Paper presented at the International Colloquium on the Fine-Scale Structure of the Atmosphere, Moscow, June 15-22 1965.

Webb, W. L. , Structure of the Stratosphere and Mesosphere. Academic Press, New York and London, 382 pp. , 1966.

Webb, W. L., W. E. Hubert, R. L. Miller and J. F. Spurling, The first meteorological rocket network. Bull. Amer. Meteor. Soc., 42, pp. 482-494, 1961.

Williamson, E. L., Gun-launched vertical probes at White Sands, Missile Range. Atmospheric Sciences Laboratory, White Sands Missile Range, New Mexico, ECOM-5030, 14 pp., 1966.

_____, and E. D. Boyer, The gun-launched meteorological sounding system. AMS/AIAA Conference on Aerospace Meteorology, Los Angeles, California, March 28-31, 1966.

Worth, J. J. B., L. A. Ripperton and C. R. Berry, Ozone variability in mountainous terrain. J. Geophys. Res., 72, pp. 2063-2068, 1967.

APPENDIX A

The Dynamic Structure of the Upper Troposphere
as Inferred from Superpressure Balloon Data

I. Introduction

From 12 to 27 September a total of eight superpressure balloon (SPB) flights were made. The release sites for the balloons were 80-100 km W to WNW of the Chalk Mountain Observatory (CMO). The balloons were tracked by the CMO radar. The mean altitude of the eight flights was 8.1 km. Extreme altitudes in the series were 3.5 and 13.7 km. Three balloon data sets will be presented in the following analysis. These are SPB_1 (released at 24 September 1969/1245 MDT), SPB_2 (24 September 1969/1700 MDT) and SPB_3 (27 September 1969/0700 MDT).

The superpressure balloon flights, as mentioned earlier, were conducted to compliment the chaff releases. The superpressure balloons provided information on atmospheric flow patterns at various levels in the mid- and upper troposphere. This information was used to obtain data relative to the orographically induced air motion. The flow pattern in the mountainous region where the balloons were flown is complicated by irregular three-dimensional flow. The wave produced flow is accordingly not easily defined even for simple west to east flow. The three cases analyzed had prevailing directions from the west and the southwest.

The relative accuracy of the SPB track is much higher than that of the chaff track at the much higher altitude. The location of a wind maximum and its altitude was determined twice within five minutes by a SPB (on the 25th of September) that did not release from its tow balloon and ascended to an altitude at which it ruptured. On the ascent the primary maximum was located at 10.59 km with $V_{(u, v)} = 25.3$ m s^{-1}. Upon descent the maximum was located at 10.46 km, $V_{(u, v)} = 25.6$ m s^{-1}.

II. Results

Of the 240 minutes of balloon data analyzed from the three flights the balloons were at a nearly constant altitude less than 30 per cent of the period. The remainder of the period the three balloons were either descending or ascending at ~ 1 m s^{-1}. This data is obviously biased by a balloon rate-of-fall or rise. The actual $\pm$ w-component of the air was determined in a fashion similar to that described earlier. These data were treated with three-minute running means.

A plot of the inferred vertical motion of the air from the balloon data is given in Figure A1. This is a plot of SPB$_1$; the wind direction was 280°--the balloon, therefore, moves from left to right across the plot. Most of the upward (+w) and downward motion (-w) is on the order of 1 to 2 m s^{-1}. Two extreme vertical velocities (w$_{max}$) are seen near the end of the flight track. These velocities are ± 8.4 m s^{-1}. This is a rather typical w-component vs. distance plot. Note that wave motion appears to be evident to some extent throughout the flight. The mean flight altitude of this balloon was 10.7 km and the total flight time 53 minutes.

The spectral analysis of the w-component of SPB$_1$ (which has been smoothed with a low-pass filter and detrended as discussed previously) is presented in Figure A2. A rather broad peak is centered at 3.8 km. A secondary peak is seen at 1.3 km. In the longer wavelength region of the spectrum ($\lambda > 1.2$ km) a spectral gap is seen at 5.2 and 1.9 km.

The spectral analysis (Figure A3) of the data set taken three hours later (SPB$_2$) shows a similarity to that of SPB$_1$. Two primary peaks are seen: one at 10.3 km, the second at 3.4 km. A secondary peak is evident at 1.2 km. Two gaps are evident: one at 5.2 and another at 1.8 km.

A spectral analysis was also performed on the 27 September data set (SPB$_3$). A broad peak is seen at 3.6 km (Figure A4). Lesser peaks are evident at 1.8 and 0.8 km. Gaps are at 2.3 and 1.0 km.
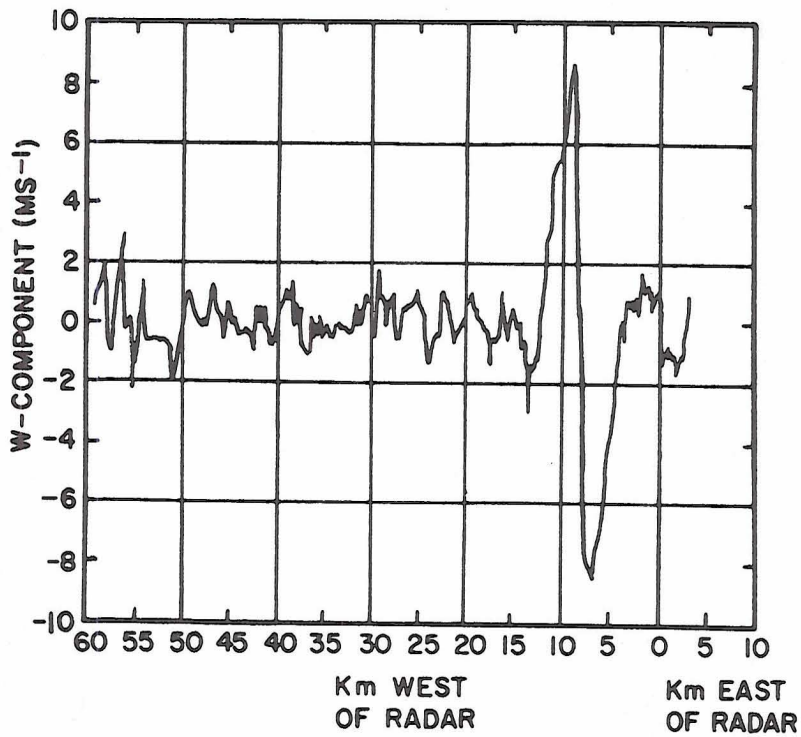
Figure A1. The vertical velocity of the superpressure balloon released at 1245 MDT on 24 September 1969 as a function of the distance from the radar receiver (see text for computation aspects).
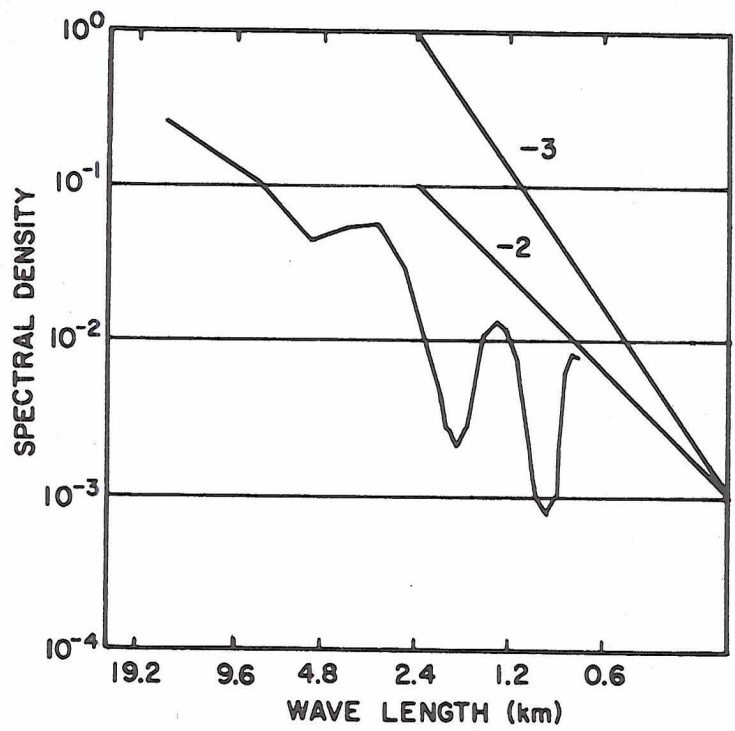

Figure A2. Normalized spectral density of the w-component of the superpressure balloon released at 1245 MDT on 24 September 1969 (SPB_1) (see text for elaboration).

Figure A3. Normalized spectral density of the w-component of the superpressure balloon released at 1700 MDT on 24 September 1969 (SPB$_2$) (see text for elaboration).

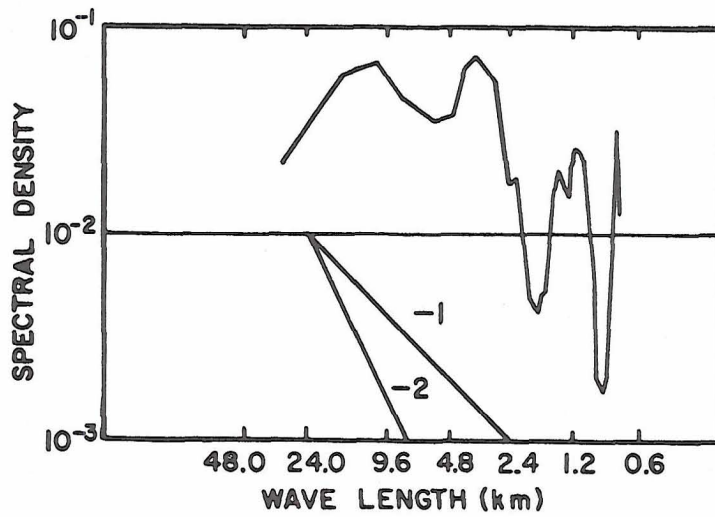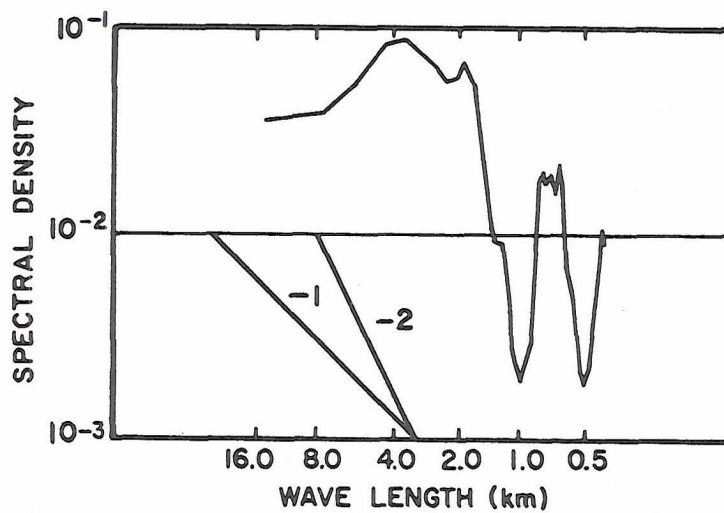Figure A4. Normalized spectral density of the w-component of the superpressure balloon released at 0700 MDT on 27 September 1969 (SPB$_3$) (see text for elaboration).

Because aliasing may have occurred at high frequencies, none of the spectra are inspected at wavelengths less than 1.0 km for SPB_1 and SPB_2 (or 0.7 for SPB_3).

III. Discussion

SPB_1 and SPB_2 data sets were collected at a period in time separated by 3 hours 15 minutes. Both sets are similar in several ways. They traveled at a mean altitude of 10.7 and 9.2 km, respectively. Their mean velocities $\bar{V}_{(u, v)}$ were identical ($\bar{V}_{(u, v)} =$ 24.0 m s^{-1}). There was a difference in the $(V_{(u, v)})_{max}$ of 36.5 vs. 28.5 m s^{-1}, respectively. Analysis of the change of height with time (dz/dt) of both data sets indicated the presence of a horizontal wavelength (λ_h) of approximately 10 km and of a vertical wavelength (λ_v) of approximately 0.2 km. $\bar{V}_{(u, v)}$ was 10.0 m s^{-1} for SPB_3 and the $(V_{(u, v)})_{max}$ only 15.2 m s^{-1}.

SPB_1 and SPB_2 spectra exhibit primary peaks at 3.8 and 3.4 km (Figures A2 and A3). SPB_3 also exhibits the primary peak at 3.6 km. It, therefore, appears as if all data sets indicate a primary mode at $\lambda \simeq 3.6$ km. Secondary peaks were seen in the spectra of SPB_1 and SPB_2 also at 1.2 km. In addition SPB_2 indicated a broad peak also at $\lambda = 10.3$ km, which is similar to the wavelength determined by the analysis of the dz/dt of SPB_1 and SPB_2.

IV. Summary

Analysis of superpressure balloon data for 24 and 27 September indicates wavelengths of approximately 1, 3.5 and 10 km. It is interesting that the 1 and 3.5 km wavelengths are in evidence in data analyzed on two different dates. This would suggest that 1 and 3.5 and perhaps 10 km are reasonable wavelengths to expect under westerly flow in this particular orographically induced flow region of Colorado. It is

obviously quite difficult to determine what resonance effect the mountains along the flight path might have on the balloon (even under strictly zonal flow).

The spectral analysis of the three sets of data indicates slopes from k^{-2} to $k^{-5/3}$ of the spectral density. Slopes of $k^{-11/5}$ have been suggested as significant of a buoyant subrange (see e. g. , Pinus et al. , 1967).

Superpressure balloon flights (SPB_1 and SPB_2) were purposely flown at different altitudes at close time intervals to determine the strength of the orographic wave at different levels in the upper troposphere. The analysis of the vertical velocity field for both data sets indicated similar magnitudes. The analysis of the non-normalized power spectra of SPB_1 and SPB_2 indicated more energy at $\lambda = 1.2$ and 3.6 for SPB_1 (10.7 km mean altitude) than SPB_2 (9.2 km mean altitude).

APPENDIX B

The Dynamic Structure of the Atmosphere from the
Mid-Troposphere to the Upper-Stratosphere
as Inferred from Closely Spaced
Ozonesonde Profiles

I. Introduction

The majority of information available on the vertical distribution of ozone in the troposphere and stratosphere before 1960 was obtained by means of the Umkehr method. In the 1960's several types of ozonesondes were developed that could give detailed ozone distributions in the atmosphere. The most recently developed ozone sensor is the Komhyr Electrochemical Concentration Cell (ECC) (Komhyr, 1969). The Komhyr ozonesonde is simple in design, lightweight, compact, and capable of providing data on an absolute scale. It derives its driving e.m.f. from a difference in electrolyte concentrations surrounding its cathode and anode. The sensor is capable of detecting a concentration of 1 part ozone in 10^9 parts of air.

Ten Komhyr ECC ozonesondes were released from the Chalk Mountain Observatory between 16 and 25 September 1969. Four ozonesondes were released at approximately 3.2 hour intervals beginning at 2213 MDT on 24 September. This section of the paper will analyze the results of the extensive atmospheric sounding project on 24 and 25 September.

II. Technique

Ozone and temperature data were obtained during ascent and descent of the instrument package. In this manner additional information can be obtained during the descent that can aid in interpretation of the ascent portion of the sounding. In the troposphere ozone values are obtained at 85 meter increments. In the stratosphere, due to an increased ascent rate of the sensor package, ozone values are

transmitted to the surface at 110 meter increments in the vertical. The ozonesonde was tracked by a radar located at the CMO. Winds were obtained in this manner and evaluated in u-, v- and w-components. The w-component is computed by subtracting the instantaneous value of the rise rate of the balloon from a running five-minute mean value of the rise rate.

A Komhyr ECC ozone continuous surface sensor was used at the CMO to monitor the surface variations of ozone. This sensor served as ground truth for the ozonesonde sensors immediately before release. Results obtained from the surface sensor are presented in Appendix C.

Special Dobson total ozone observations were taken at Boulder, Colorado during this period. The ozonesonde vertical profiles were integrated and compared with the total ozone measured by the Dobson Spectrophotometer. All ozone data presented herein are corrected to the total values accordingly.

III. Results

The only orographically produced gravity wave clouds observed between 12 and 25 September were seen on the evening of the 24th and were still visible on the morning of the 25th.

There was much evidence of gravity wave activity in each ozonesonde sounding. In fact during the 12-hour period in which four ozonesondes were released, it appears as though the gravity wave structure over the observatory was very nearly stationary. This becomes evident when the vertical velocities of the four ozonesondes (O_{31} released on 24 September 1969 at 2213 MDT; O_{32}, 25 September, 0138 MDT; O_{33}, 0534 MDT; O_{34}, 0817 MDT) are examined. The distribution of the w-component for O_{31} (Figure B1a) suggests that the balloon passed through several gravity waves as it ascended. It appears as if the ozonesonde passed through 6-7 waves between 4 and 19 km.
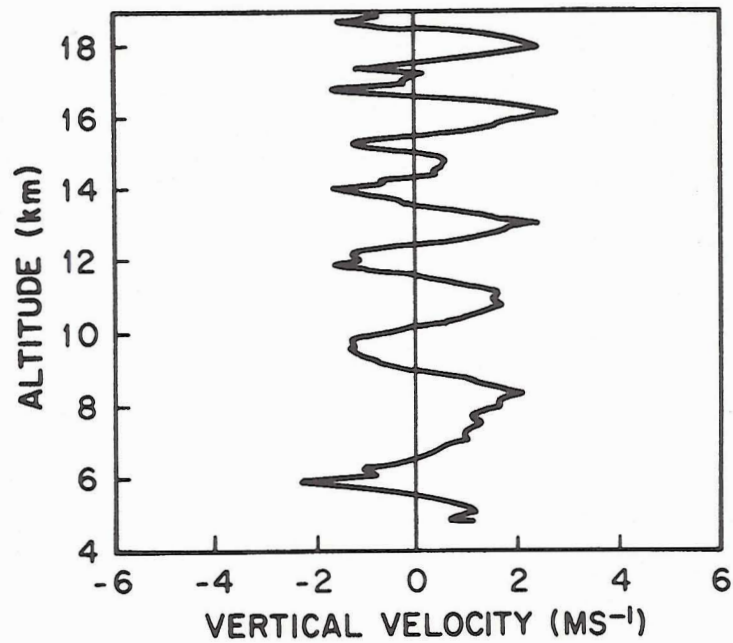
Figure B1a. Vertical velocity as inferred from ozonesonde O_{31} released at 2213 MDT on 24 September 1969.
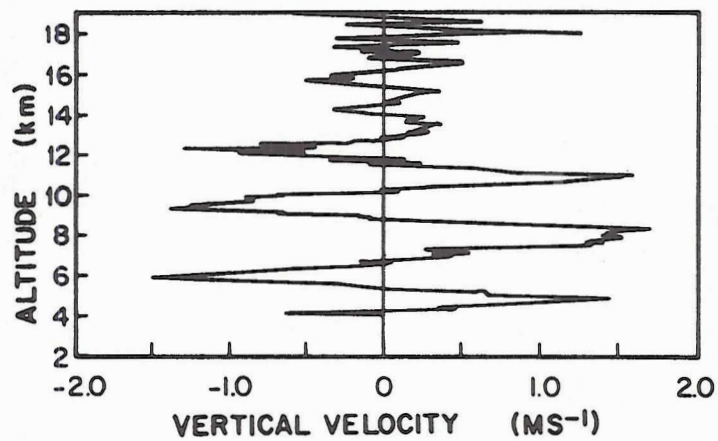

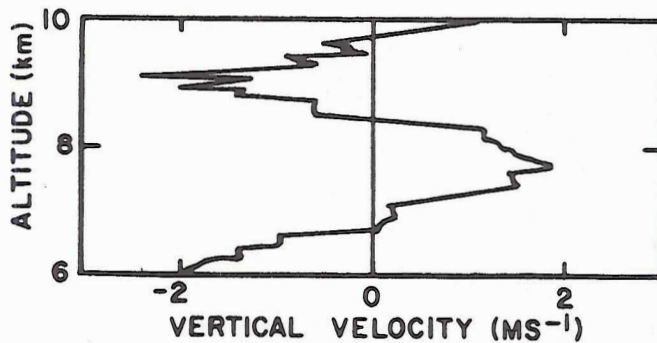Figure B1b. Same as B1a, except (O_{32}) 0138 MDT, 25 September 1969.

Figure B1c. Same as B1a, except (O_{33}) 0534 MDT, 25 September 1969.

The ozonesonde package was 45 km from the station by the time it reached an altitude of 19 km. It passed through the wave structure at an angle of approximately 30° against the horizontal. Thus, one is not viewing the wave structure inferred from the vertical motion, as it was directly over the observatory, but along a slanting line from the station.

Figures B1b, B1c and B1d depict the vertical velocities inferred from ozonesonde data sets O_{32}, O_{33} and O_{34}. A radar tracking problem existed from 10 to 23 km during the ascent of O_{33}, therefore Figure B1c is terminated at 10 km. Even a cursory examination of Figures B1a, b, c, d indicates a similarity in velocity magnitudes and locations of positive and negative vertical velocity ($\pm$ w) layers. Figure B1a indicates that $w = -2.2 \text{ m s}^{-1}$ at 5.9 km. Figure B1b shows $w = -1.6 \text{ m s}^{-1}$ at 6.0 km. The following two figures indicate vertical velocities of -2.0 and -1.3 m s^{-1}, both at 6.0 km.

As can be seen by examination of Figure B1a, there is a vertical wavelength of approximately 4 km from 6 to 10 km and approximately 2 km from 10-19 km. Examination of the following three ozonesonde (Figures B1b, c, d) vertical velocity fields indicates variations of similar magnitude at essentially the same altitudes as those of the O_{31} data set. There are slight variations in the intensity of the vertical velocities and the location of the layers. This would seem to indicate that the wave motion is only quasi-stationary. But considering the remarkable matching, nearly point for point, of the vertical velocity field along the z-coordinate it is reasonable to assume that the situation was one of near stationarity.

There are quasi-regular oscillations in the vertical profile of $V_{u, v}$ for the O_{31} data set (Figure B2). Oscillations similar to this have been reported in the horizontal wind field in the troposphere and lower stratosphere that were associated with gravity waves (Lovill and Miller, 1968).
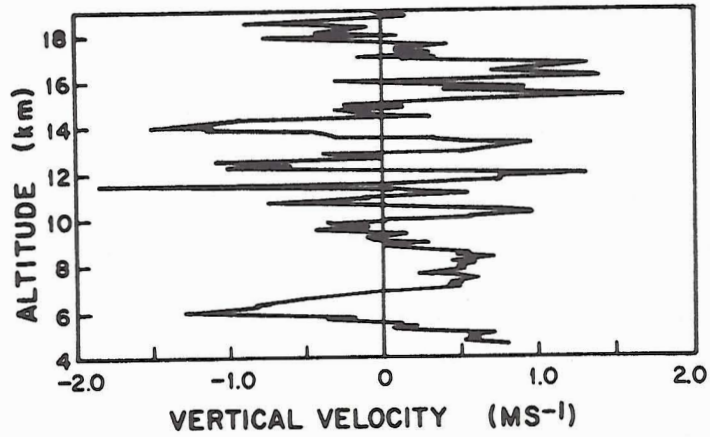
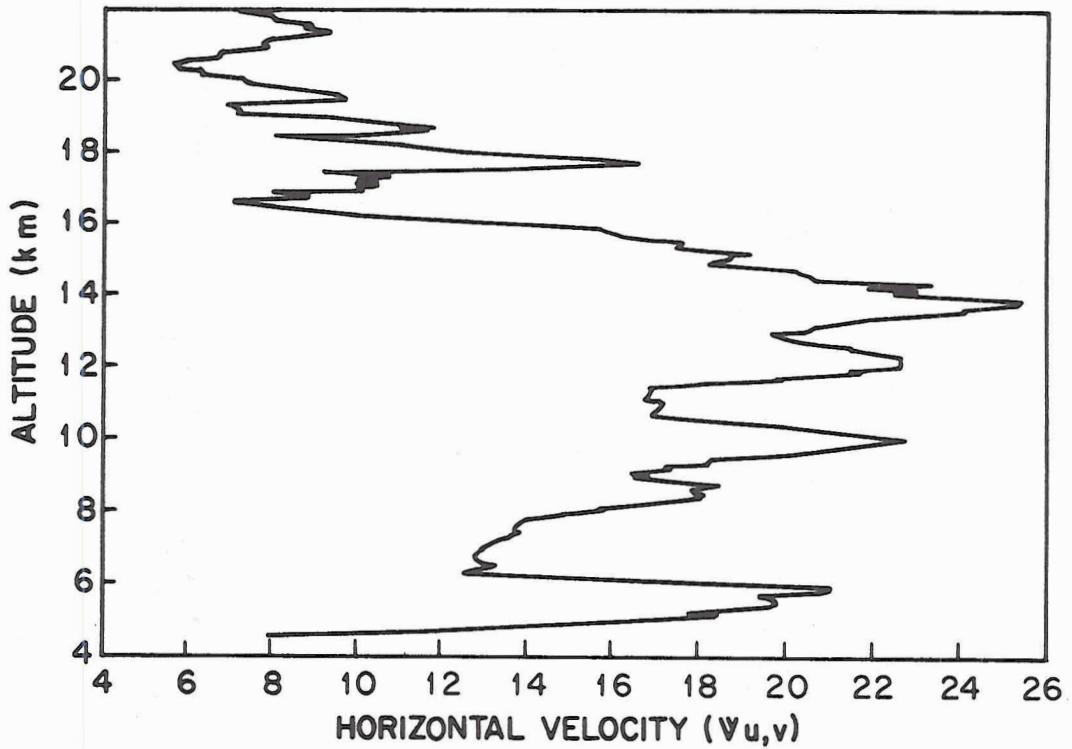Figure B1d. Same as B1a, except (O_{34}) 0817 MDT, 25 September 1969.

Figure B2. Horizontal velocity vs. altitude, ozonesonde O_{31} released at 2213 MDT on 24 September 1969.

Since the vertical structure of the vertical velocity changed little (the u- and v-wind component in the vertical also maintained a stationary structure), it was decided to present the <u>mean</u> structure of the different parameters in the vertical, averaged over the four soundings. The following figures are computer processed, average profiles of $V_{u,v}$ (Figure B3), u- and v-components (Figure B4), ozone partial pressure in nanobars (Figure B5) and the temperature (Figure B6).

Figure B3, showing the vertical variations of the horizontal wind, indicates a low level velocity maximum of 29.3 m s^{-1} less than 2000 meters above the station. Since the wind at the observatory was calm, this indicates a shear of ~15 m s^{-1} km^{-1}. Also note the minimum of 3.6 m s^{-1} at 7 km and the secondary maximum of 26 m s^{-1} which is located ~3 km below the tropopause.

Figure B4 depicts the u- and v-component fluctuations in the vertical. Notice that the flow is strongly from the west in the low level maximum with a u-component 50 per cent larger than the v-component.

Figure B5 represents the ozone distribution in the vertical. The large scale maximum in the ozonosphere is at 25.8 km. The partial pressure at this altitude is 142 ηb which agrees with other measurements for this period (see Bojkov, 1967; Hering and Borden, 1967). The "ozone tropopause" is well defined at 16.7 km. The ozone tropopause has been defined as the altitude at which the ozone partial pressure lapse rate changes from a slow increase with height to a very rapid increase with height (Lovill, 1968). This boundary marks well the separation between the high concentrations of stratospheric ozone and the low concentrations of ozone in the troposphere. During the present measurements it corresponds exactly with the temperature tropopause (Figure B6).

A very interesting feature in the computer-averaged vertical distribution of ozone is seen in the lower troposphere. At 5.7 km
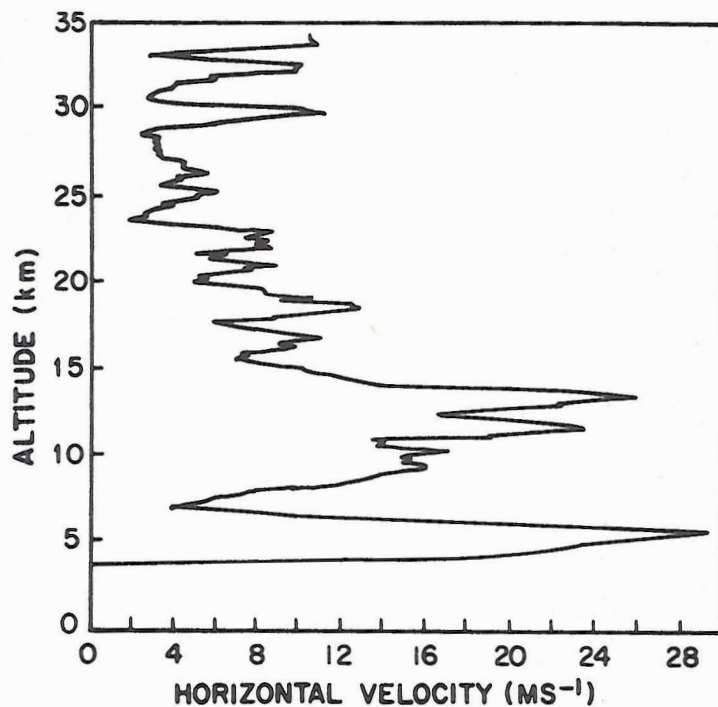
Figure B3. Average profile of $\mathbb{V}_{u,v}$ vs. altitude for four data sets.
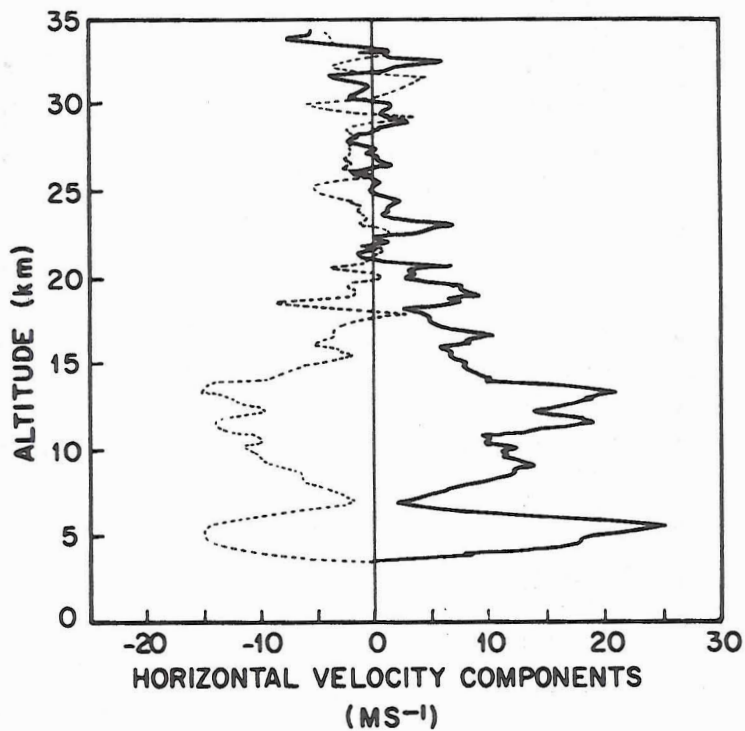

Figure B4. Average profile of the u- and v-components vs. altitude for four data sets (solid line is E-W component--a positive value is from the West; dashed line is N-S component--a negative value is from the North).
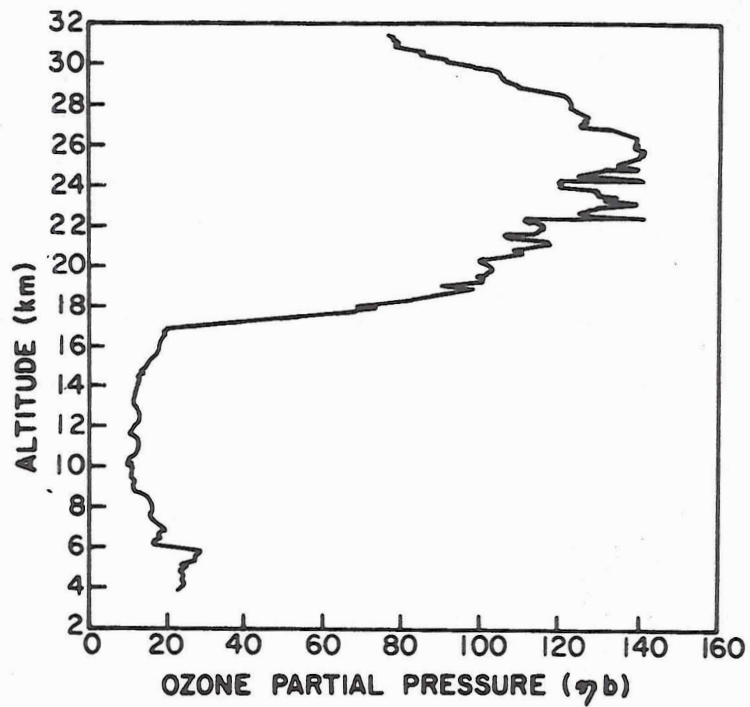
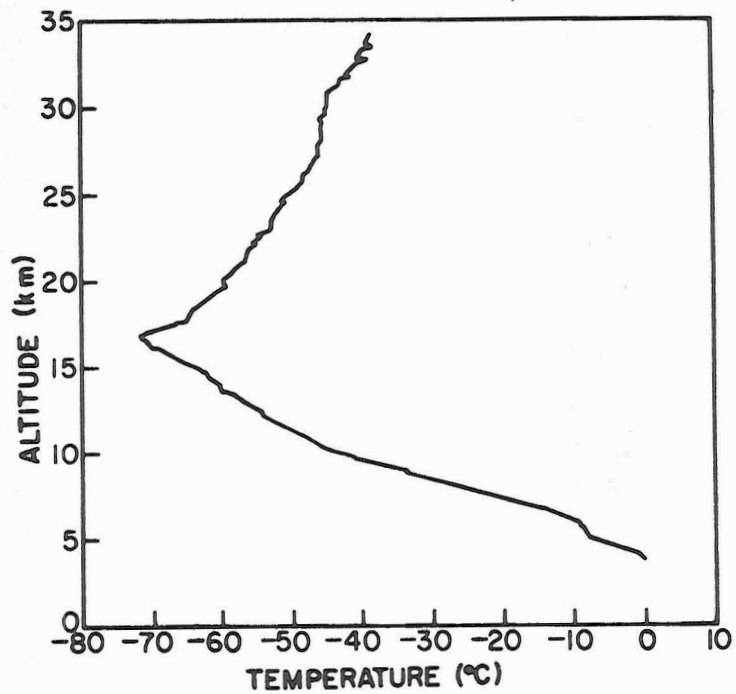Figure B5. Average vertical distribution of ozone for four data sets.

Figure B6. Average vertical distribution of temperature for four data sets.

there is a maximum in ozone of 27 η b. This maximum may be com-
pared with the horizontal and vertical velocity fields. The low-level
velocity maximum at 5.5 km (Figure B3) is located very near a region
of vertical convergence as inferred from analysis of the vertical velo-
city. The vertical velocity at 4.7 km is +1.4 m s^{-1} and at 6.2 km is
-0.9 m s^{-1}. The region above and below the 5 to 6 km layer has an
adiabatic lapse rate (Figure B5). However, the layer from 5 to 6 km
indicates a near-isothermal lapse rate in the mean profile (Figure
B5). The slight inversions present in the individual profiles are not
seen in the computer-averaged profile. The inversions are merely
reflected there as a near-constant temperature.

It appears that the ozone maximum correlates well with a low
level velocity maximum, an area of vertical convergence, and an
isothermal temperature lapse rate. We suggest that this ozone maxi-
mum and corresponding parameter variations are the direct result of
a quasi-stationary gravity wave structure. This wave structure was
not absolutely stationary during the 12-hour period. This is suggested
from analyses of the individual ozone profile variations. There are
indications that the low level ozone maximum lowered in time during
the night and early morning hours. The lowering amounted to less
than one kilometer during this period. This would suggest some move-
ment of the gravity wave, however slight.

A similar situation with a maximum of ozone at approximately
one kilometer off the surface has been observed under winter condi-
tions in the San Francisco region (Lovill and Miller, 1968). In that
case, as well as the Colorado case, the maximum of ozone was asso-
ciated with a wind maximum and a temperature inversion.

IV. Summary

Several ozonesondes were released at approximately three-hour
intervals from a high mountain observatory. Ozone, temperature and
the u-, v- and w-components of the wind were measured. Analysis

of the ozone and wind data revealed a near stationary gravity wave structure above the station during a twelve-hour period.

A maximum of ozone was measured at two kilometers above the station. The maximum was associated with a slight temperature inversion as well as a wind maximum of 29 m s^{-1}.

APPENDIX C

The Variability of Ozone at a High Mountain Location

The earth's surface is a very effective sink for ozone (Dütsch, 1946; Paetzold, 1955; Junge, 1963; Aldaz, 1969; Regener, 1969). The normal ozone variability during the day at a location other than in mountainous terrain would indicate a maximum in the afternoon and a minimum in the early morning. This is because a normal wind minimum during the early morning hours results in destruction of ozone in the lowest layer near the surface. However, during the day the inversion that had existed during the early morning has either been destroyed or raised considerably by convective activity. The result is that the ozone layer near the surface is being continuously replenished with air rich in ozone from above.

During the three-week period of the investigation an ozone sensor was operating nearly continuously at the Chalk Mountain Observatory. The instrument was a Komhyr ECC ozone sensor (described previously in Appendix B).

Ozone values at one-half hour intervals were selected from the sensor recorder. The data were processed by computer. Figure C1 is the computer-produced hourly average of the ozone density (as well as the concentration and partial pressure).

Immediately evident in a sine-like curve of the mean variation during the day. A maximum ozone value is seen at 0530 MDT and a minimum value at 1430 MDT.

Also immediately evident is the fact that the ozone variation at the Chalk Mountain Observatory is 180° out-of-phase with the observed ozone fluctuations mentioned above. The maximum in the early morning and the minimum in the afternoon has been observed at other mountainous stations. Worth et al. (1967) obtained similar observations on a mountain top in western North Carolina that was considerably lower than the Chalk Mountain Observatory.
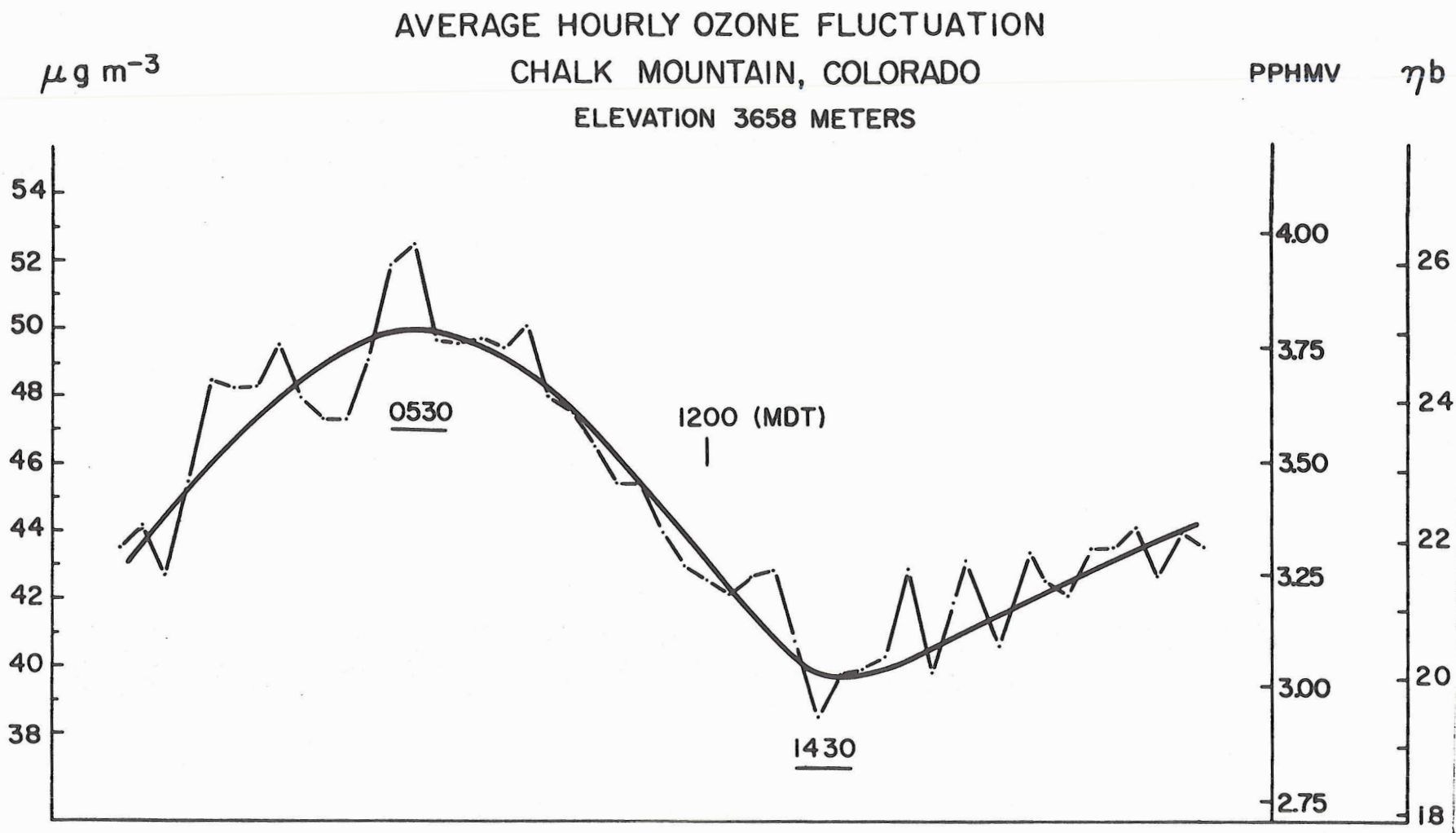
Figure C1. The hourly ozone fluctuation at The Chalk Mountain Observatory. The solid line is a best fit curve through the data points.

These data are unique in that they are the highest altitude record in the continental United States. The time-location of the maximum and minimum during the day suggests, of course, a condition of a deeper mixing layer, with more turbulence, and with more ozone being brought to the surface during the morning hours at the mountain top.

However another fact is to be considered. Because of a differential heating of the slopes of the mountain and the free air at the same altitude, an upslope wind (valley wind) develops. At night the differential heating allows the opposite to occur and a downslope wind occurs.

It is therefore suggested that at the Chalk Mountain Observatory during the day air is brought to the mountain top that, as a rule, has travelled upward along the sides of the mountain. This ozone-poor air would account for the distinct minimum of ozone in the afternoon. At night, however, the downslope wind would import air rich in ozone from aloft.